Faraday Discussions

Accepted Manuscript

This manuscript will be presented and discussed at a forthcoming Faraday Discussion meeting. All delegates can contribute to the discussion which will be included in the final volume.

Register now to attend! Full details of all upcoming meetings: http://rsc.li/fd-upcoming-meetings

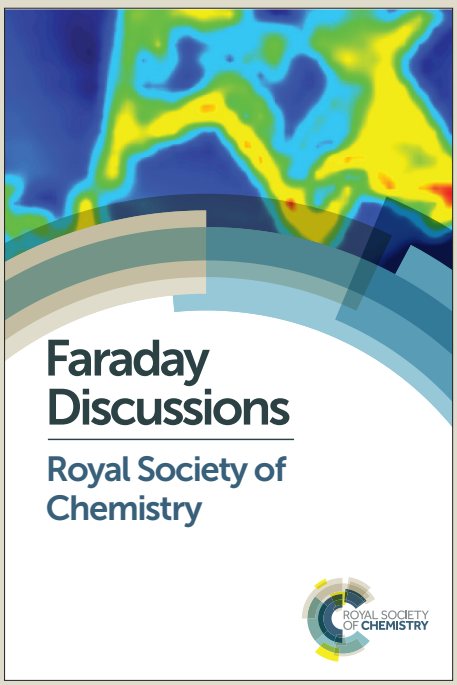

This is an *Accepted Manuscript*, which has been through the Royal Society of Chemistry peer review process and has been accepted for publication.

Accepted Manuscripts are published online shortly after acceptance, before technical editing, formatting and proof reading. Using this free service, authors can make their results available to the community, in citable form, before we publish the edited article. We will replace this *Accepted Manuscript* with the edited and formatted *Advance Article* as soon as it is available.

You can find more information about *Accepted Manuscripts* in the Information for Authors.

Please note that technical editing may introduce minor changes to the text and/or graphics, which may alter content. The journal's standard Terms & Conditions and the Ethical guidelines still apply. In no event shall the Royal Society of Chemistry be held responsible for any errors or omissions in this *Accepted Manuscript* or any consequences arising from the use of any information it contains.

ROYAL SOCIETY OF CHEMISTRY

www.rsc.org/faraday_d

Raman spectroscopy for cytopathology of exfoliated cervical cells

Ramos IR[1,2], Meade AD[2], Ibrahim O[1,2], Byrne HJ[3], McMenamin M[4], McKenna M[4], Malkin A[5], Lyng FM[1,2]

[1]DIT Centre for Radiation and Environmental Science, FOCAS Research Institute, Dublin Institute of Technology, Kevin St, Dublin 8, Ireland

[2]School of Physics, Dublin Institute of Technology, Kevin St, Dublin 8, Ireland

[3]FOCAS Research Institute, Dublin Institute of Technology, Kevin St, Dublin 8, Ireland

[4]Cytopathology Department, Altnagelvin Hospital, Western Health and Social Care Trust, Derry, Northern Ireland, United Kingdom

[5]School of Biological Sciences, Dublin Institute of Technology, Kevin St, Dublin 8, Ireland

*Corresponding author:

Prof. Fiona M. Lyng

DIT Centre for Radiation and Environmental Science,

FOCAS Research Institute

Dublin Institute of Technology

Kevin St

Dublin 8

Ireland

t: +353 1 4027972

f: +353 1 4027904

e : fiona.lyng@dit.ie

Keywords

Raman spectroscopy, cervical cancer, cervical intraepithelial neoplasia (CIN), low grade squamous intraepithelial lesion (LSIL), high grade squamous intraepithelial lesion (HSIL), cytopathology, exfoliated cells

Abstract

Cervical cancer is the fourth most common cancer affecting women worldwide but mortality can be decreased by early detection of pre-malignant lesions. The Pap smear test is the most commonly used method in cervical cancer screening programmes. Although specificity is high for this test, it is widely acknowledged that sensitivity can be poor mainly due to the subjective nature of this test. There is a need for new objective tests for the early detection of pre-malignant cervical lesions. Over the past two decades, Raman spectroscopy has emerged as a promising new technology for cancer screening and diagnosis. The aim of this study was to evaluate the potential of Raman spectroscopy for cervical cancer screening using both Cervical Intraepithelial Neoplasia (CIN) or Squamous Intraepithelial Lesion (SIL) classification terminology. ThinPrep® Pap samples were recruited from a cervical screening population. Raman spectra were recorded from single cell nuclei and subjected to multivariate statistical analysis. Normal and abnormal Thinprep samples were discriminated based on the biochemical fingerprint of the cells using Principal Component Analysis (PCA). Principal Component Analysis – Linear Discriminant Analysis (PCA-LDA) was employed to build classification models based on either CIN or SIL terminology. This study has shown that Raman spectroscopy can be successfully applied to the study of routine cervical cytology samples from a cervical screening programme and that use of CIN terminology resulted in improved sensitivity for high grade cases.

Introduction

Cervical cancer is the fourth most common cancer in women worldwide, accounting for an estimated 528,000 new cases and 266,000 deaths in 2012.[1] However, the mortality associated with cervical cancer can be significantly reduced if this disease is detected at the early stages of development or at the pre-cancer stage, termed cervical intraepithelial neoplasia (CIN). Cervical cancer mainly affects younger women, about 60% of cases occurring in women under 50 years of age. Persistent infection with Human Papillomavirus (HPV) (such as high risk HPV types 16 and 18) is accepted as the major cause for the development of cervical pre-cancer and cancer.[2] Other risk factors include smoking, immunosuppression, long term use of oral contraceptives and socioeconomic status.[3]

Cervical cancers are usually preceded by a long phase of pre-invasive disease. This phase is characterised microscopically as a sequence of events progressing from cellular atypia to various grades of dysplasia or CIN before progression to invasive carcinoma. Introduced in 1968, CIN is the most common terminology for cervical histology. It is a three-tiered system, divided into grades 1, 2 and 3, whereby CIN 1 corresponds to mild dysplasia, CIN 2 to moderate dysplasia, and CIN 3 corresponds to both severe dysplasia and carcinoma *in situ*.[4] In cytology, the British Society for Clinical Cytology (BSCC) reporting system for cervical cancer refers to different grades of dyskaryosis which relate to the three-tiered CIN terminology with CIN 1 corresponding to mild dyskaryosis, CIN 2 corresponding to moderate dyskaryosis and CIN 3 to severe dyskaryosis. Since then, advances in HPV research and liquid based cytology led to the introduction of the Bethesda System in the United States of America.[5] According to this nomenclature, squamous intraepithelial lesion (SIL) encompasses a range of non-invasive cervical epithelial abnormalities, comprising low grade (LSIL) and high grade lesions (HSIL). Low grade lesions correspond to cellular changes associated with the HPV cytopathic effect (koilocytotic atypia) and mild dysplasia (CIN 1), whereas high grade lesions correspond to moderate dysplasia, severe dysplasia, and carcinoma *in situ* (CIN 2 and 3). The two-tiered terminology of SIL is the standard reporting system for cervical cytology used in many

screening programmes across developed countries. Since 2012, the College of American Pathologists and the American Society for Colposcopy and Cervical Pathology has recommended a uniform terminology to describe the histology of HPV-associated squamous disease across all anogenital sites. The two tiered terminology of LSIL and HSIL is recommended, as it reflects the biology of transient HPV infections and persistent precancerous lesions.[6] More recently, the BSCC terminology was also revised to comprise the terms low grade, high grade with the option of high grade dyskaryosis being further reported as moderate or severe.[7] Table 1 summarises the different classification systems.

The gradual progression of cervical cancer can allow the detection of dysplastic changes before invasive cancer develops through cervical cancer screening programmes. These screening programmes are common in developed countries, greatly reducing the mortality rates due to cervical cancer, but are not yet implemented in developing countries due to lack of infrastructure and funding. The Papanicolaou (Pap) test is the most common screening method for cervical cancer and its precursor lesions.[8] The advantages of the Pap test are that it is non-invasive, inexpensive and widely accepted. However, although it can have high specificity of up to 95-98%, sensitivity rates can vary from 74 to 96%, due to sampling, technical and/or interobserver errors which are associated with the subjective nature of cytological screening.[9] There is, therefore, a need for new objective screening tests for cervical cancer.

Over the past 15 years, excellent sensitivity and specificity values have been reported using vibrational spectroscopy, InfraRed (IR) and Raman, for the diagnosis of a wide range of cancers, including breast, prostate, oesophageal, colon, lung, oral and cervical cancer.[10-12] IR spectroscopy is based on the absorption of infrared radiation by the sample and the fact that molecules absorb specific frequencies of the incident light which are characteristic of their structure. Raman spectroscopy is an optical method based on inelastic light scattering. The sample is illuminated by

monochromatic laser light and interactions between the incident photons and molecules in the sample result in scattering of the light. The coupling of the light generates vibrations within the material which are characteristic of the chemical structure and the energy of the scattered light is reduced by an amount equal to the energy of the vibrational energy. Thus, the positions, relative intensities and shapes of the bands in a Raman spectrum carry detailed information about the molecular composition of the sample.

A number of papers by Wong and co-workers in the early 1990's showed significant differences in cervical cytology cells between normal, pre-cancer and cancer samples using IR spectroscopy.[13-16] However, these initial studies recorded spectra from cell pellets rather than from individual cells and a number of confounding factors such as neutrophils, endocervical columnar cells, metaplastic cells, cervical mucus and debris were subsequently identified.[17] Similar confounding factors, such as inflammation, metaplasia, hormonal changes, metabolic activity, blood and mucus, were identified by other groups.[18-22] Nevertheless, an early study by Cohenford and Rigas[23] reported an important finding that morphologically normal exfoliated cells from women with dysplasia or cancer exhibited extensive IR spectral changes. This finding was confirmed by Schubert *et al.*[24], who showed spectral changes in cytologically normal cells in dysplastic samples, most likely due to HPV infection. Significant overlap was observed between negative, LSIL and HSIL cases using ATR—FTIR spectroscopy with maximal overlap between negative and LSIL cases[25]. but a more recent study showed that cervical pre-cancer is more accurately identified when histology rather than cytology is used as the gold standard to classify the samples.[26]

There are relatively fewer studies on cervical cytology using Raman spectroscopy, most likely because of the issues with confounding factors. Vargis *et al.*[27] showed that Raman spectroscopy could classify HPV-positive and HPV-negative cytology samples with an accuracy of 98.5%. Rubina *et al.*[28] reported a classification accuracy of ~80% using Raman spectroscopy to distinguish between normal and cervical cancer cytology samples. Cytology samples were treated with red blood cell lysis buffer prior to Raman acquisition as the spectra of cervical cancer samples were dominated by blood features. Both

of these studies used cell pellets rather than recording Raman spectra from individual cells and this probably resulted in the relatively low classification accuracy in the study by Rubina *et al.* due to sample heterogeneity. A recent study by Bonnier *et al.*[29] presented new methods for recording Raman spectra from ThinPrep cervical cytology samples. Pre-treatment of the slides with hydrogen peroxide to clear blood residue contamination before Raman recording was shown to minimise variability within the data sets resulting in the collection of highly reproducible data with clear discrimination between negative cytology and CIN cytology. All data was recorded on glass ThinPrep slides which are currently used for clinical cervical cytology rather than spectroscopic substrates such as calcium fluoride substrates which are commonly used in biospectroscopy research studies. Although these substrates reduce the presence of confounding contributions of the substrate, they are significantly more expensive which may prohibit clinical applications.[30]

The aim of this study was to evaluate the potential of Raman spectroscopy for cervical cancer screening using routine cervical cytology samples from a cervical screening programme. Cytology samples were classified according to both CIN and SIL terminology and Raman classification models compared.

Experimental

Sample Collection and slide preparation

166 unstained smear samples in ThinPrep™ slides were obtained from the Western Health & Social Care Trust Altnagelvin Hospital, Northern Ireland, with the approval of the Research Ethics Committee Northern Ireland.

Smears were collected, processed via the ThinPrep™ method, Papanicolau (Pap) stained and screened in the hospital by specialised personnel according to the guidelines in practice. A total of 88 negative, 35 CIN1 (or 35 LSIL) and 21 CIN2 and 22 CIN3 (or 43 HSIL) cases were randomly selected and included in this study. Each case represents a sample from an individual patient.

One duplicate slide of each selected case was prepared using the ThinPrep™ method, fixed in 100% ethanol and air-dried. The samples were sent to Dublin Institute of Technology for Raman analysis. Before recording, each slide was pre-treated with hydrogen peroxidase (H_2O_2), as per an in-house protocol[29] to remove any contaminating blood and debris.

Raman Microspectroscopy

Raman measurements were performed using a HORIBA Jobin Yvon XploRA™ system (Villeneuve d'Ascq, France), which incorporates an Olympus microscope BX41 equipped with a x100 objective (MPlanN, Olympus, N.A. 0.9) and a 532nm diode laser source. To avoid any photo damage to the sample, the power of the laser was set at 50%. The confocal hole was set at 100μm and the 1200 lines/mm grating was used, which gave a spectral dispersion of ~3 cm^{-1} per pixel. The backscattered light was collected using an air-cooled CCD detector (Andor, 1024 x 256 pixels) and the spectrometer was controlled by Labspec V5.0 software. The system was calibrated to the 520.7 cm^{-1} spectral line of silicon.

Raman signals from each cell nucleus were integrated twice for 30 seconds in the spectral range of 400-1800cm^{-1}. Spectra from a minimum of 10 cell nuclei were recorded per sample, depending on

the quality of each slide. The data is presented as the average of all 10 cellular spectra recorded from each individual patient.

Data analysis

Data analysis was performed in Matlab [Mathworks, CA, USA] according to protocols developed in house.[31] Pre-processing of the raw Raman spectra included the application of a Savitsky-Golay filter (5^{th} order, 13 points) to smooth the spectra and the subtraction of the glass background according to an in house non-negative least squares (NNLS) model.[32] The data set has also been corrected for baseline and vector normalized to facilitate comparison before principal component analysis (PCA) was employed to highlight the variability existing in the spectral data set recorded. Principal component analysis – linear discriminant analysis (PCA-LDA) was also employed to generate a classification model based on the features highlighted by PCA analysis. The optimal number of principal components (PCs) to generate the PCA-LDA model was established and 10 fold cross-validation used to test it. Furthermore, leave one out cross validation (LOOCV) was then used to evaluate the performance of the PCA-LDA classification model and sensitivity and specificity rates were calculated for both SIL and CIN classifications.

Results

Mean Raman spectra of cervical cytology samples in the fingerprint region of 400-1800 cm^{-1} are shown in figure 1a. The samples are presented according to the SIL classification system; negative, LSIL and HSIL. The main peaks are indicated and assignments are listed in table 1.[33] The mean spectra of negative, LSIL and HSIL samples show similar features, the main differences being observed around the 1318/1339 cm^{-1} region, in which the ratio of the intensities of these two peaks increases from negative to LSIL and HSIL samples as shown in figure 1b.

To further highlight any differences between the spectral profiles of the samples, PCA was employed. Figure 2a shows the PCA scatterplot for all SIL classified samples. From the PCA scatterplot, it can be seen that negative (green), LSIL (magenta) and HSIL (black) samples are separated according to the first (PC1) and second (PC2) principal components which account respectively for 76.81 % and 7.548 % of the variance explained in the dataset. The loadings for PC1 and PC2 are shown in figure 2b and c. The negative samples seem to separate from the LSIL samples according to PC1, negative samples having more DNA (~814 cm^{-1}), protein and lipids (1307, 1446, 1453 cm^{-1}), Amide III (1242 cm^{-1}) and I (1690 cm^{-1}) also featuring prominently. Furthermore, the negative samples separate to a large extent from the HSIL samples according to PC2. Negative samples show stronger Amide III (1243, 1375 cm^{-1}) and protein/lipid (1339 cm^{-1}) features, whereas HSIL samples display stronger Amide I (1606 cm^{-1}) and Amide II (1544 cm^{-1}). In addition, the PC2 loading also highlights differences in nucleic acids, the features at 1458 and 1485/7 cm^{-1} being more prominent in the spectra of negative samples. DNA features at 481 and 786 cm^{-1} are more prominent in negative samples, whereas the feature at 893 cm^{-1} is more prominent in HSIL samples. Similarly, phosphate and phosphodiester bonds at 812 cm^{-1} are more prominent in HSIL samples, whereas those at 1087-9 cm^{-1} are more prominent in negative samples. The separation between LSIL and HSIL samples results from a combination of PC1 and PC2. Taking the PC1 and PC2 assignments for the negative samples as a reference, the LSIL samples have a similar PC2 profile to the negative samples whereas the HSIL samples have a similar PC1 profile to the negative samples.

The PCA results suggest that significant differences can be found in the Raman spectral profile of cell nuclei to distinguish between negative, LSIL and HSIL samples. PCA-LDA was therefore used to generate a classification model based on the features highlighted by PCA analysis.Results showed that a model with 12 PCs was best for LDA. Leave one out cross validation (LOOCV) was then used to evaluate the performance of the PCA-LDA classification model and sensitivity and specificity rates are shown in table 3.

Apart from the HSIL sensitivity, the performance of the PCA-LDA model is quite encouraging, all sensitivity and specificity values being above 90%. Sensitivity is also called the true positive fraction and accounts for the number of reported positives that are correctly identified as such. As the HSIL group consists of samples previously classed by the CIN classification system as CIN 2 and CIN 3, it was decided to re-evaluate the data according to the CIN classification.

Figure 3a shows the mean Raman spectra of CIN 2 and CIN 3 samples. Only small differences can be observed; a peak at 1246 cm^{-1} assigned to Amide III and one at 1417 cm^{-1} assigned to C=C stretching in a quinoid ring are only observed in CIN 2 spectra whereas the CH_3/CH_2 twisting or bending mode of lipid/collagen at 1309 cm^{-1} is only evident in CIN 3 spectra.

PCA was performed on the dataset according to the CIN classification and the PCA scatterplot is shown in figure 3b. CIN2 (red) is not clearly separated from the other sample groups but, along PC1, it can be seen distributed between CIN 3 (black) and CIN 1 (magenta) samples. To further elucidate the differences between all CIN samples, pairwise PCA was performed on spectra from CIN 1, CIN 2 and CIN 3 samples and the results are shown in figure 4. CIN 1 and CIN 2 samples show some overlap but there is some separation along PC1 (figure 4a). PC1 is positively dominated by Amide I (1663 cm^{-1}) and other protein features (~1309, 1449 cm^{-1}), as shown in figure 4b, indicating that these are more prominent in CIN2 samples. Similarly, CIN 1 and CIN 3 show some overlap but there is some separation along PC1 (figure 4c). In this case, PC1 is also positively dominated by Amide I (1669 cm^{-1}) and other protein features (~1308, 1453 cm^{-1}), as shown in figure 4d, indicating that

these are more prominent in CIN 3 samples compared to CIN 1 samples. CIN 2 and CIN 3 samples show reasonably good separation with some overlap along PC3 (figure 4e). PC3 is positively dominated by nucleic acid features at 722, 786, 810 and 850 cm^{-1} and Amide III at 1242 cm^{-1}, which are more intense in the spectra of CIN 3 samples, whereas Amide I features at 1651 cm^{-1} and C-H vibration of proteins and lipids at 1449 cm^{-1} are more prominent in the Raman spectra of CIN 2 samples.

For the PCA-LDA of the dataset according to the CIN classification, a model with 14 PCs was best for LDA and, similar to the SIL classification analysis, LOOCV was then used to evaluate the performance of the PCA-LDA classification model and sensitivity and specificity rates are shown in table 4. All sensitivity and specificity values of the PCA-LDA model were greater than 90%.

Discussion

In this study Raman spectra were acquired from the nuclei of single cells of Thinprep cervical cytology specimens on glass slides. Recording spectra from the cell nuclei may explain the similarity between the average spectrum of the different sampling groups, as biochemically the nucleus of a normal cell and the nucleus of an abnormal cell are similar. Several studies have reported increases in nucleic acids in abnormal tissue samples compared to normal tissue samples.[34-37] Abnormal tissue is characterised by increased cell proliferation rates and therefore more cells are expected to be detected/scanned (per area) on abnormal samples, resulting in substantial differences compared to normal tissue samples. In the present study, despite targeting the nuclei of the cells, it is mainly protein features which seem to discriminate the groups, although some differences in nucleic acid features were also observed. It should be noted that the Raman signals will have some degree of contribution from the cytoplasm of the cells as the laser passes through the cell to reach the nucleus.

A previous study of cervical cytology specimens, although conducted on cellular pellets rather than cell monolayers, reported Amide I (1660 cm^{-1}), ∂CH_2 (1450 cm^{-1}) and phenylalanine (1002 cm^{-1}) as the main features dominating the Raman spectra of negative samples.[28] After a treatment to remove blood from the samples an increase in protein content (at 1006, 1450 and 1660 cm^{-1}) and changes in their secondary structure due to positive Amide III bands were found. This adds to the case that instead of concentrating on increases and/or decreases in DNA and nucleic acids, Raman spectroscopy profiling for cervical cancer diagnosis can benefit from a better understanding of protein assignments.

A change in ratio at 1318/1339 cm^{-1} was also observed for negative, LSIL and HSIL cases, suggesting a decrease in the lipid/protein to guanine ratio in LSIL and HSIL samples, which may result from either a reduction of lipids/proteins and/or an increase in the nucleic acid (guanine) content of these samples.

The sensitivity and specificity values for the PCA-LDA models generated in this study were extremely high, especially when compared with Pap screening.[9] All values in the CIN classification were greater than 90% and with the exception of the HSIL sensitivity of ~ 86%, the same was also observed for the SIL classification. The lower HSIL sensitivity value of 86% seems to suggest that the CIN 2 cases are from a heterogeneous group and perhaps some of the samples diagnosed as such might be biochemically closer to CIN 1 than CIN 3 and therefore may not be correctly classified as HSIL.

In fact, a recent study by Doorbar *et al.*[38] which investigated the correlation of CIN classification and HPV infection status suggested that some reported CIN 2 cases, when analysed by an immunohistochemistry panel of P16INK4a, MCM and HPV-encoded E4, in fact group with CIN 1 rather than CIN 3 cases. The study showed that the combination of identification of surrogates of high-risk HPV E6/E7 activity (P16INK4a and MCM), together with the detection of the abundant HPV-encoded E4 protein, was able to identify both transient and transforming lesions. This approach not only allowed to distinguish true papillomavirus infections from similar pathologies but also to divide the heterogeneous CIN 2 category into those that are CIN 1-like with transient HPV infection expressing E4, and those that do not express E4 and therefore are more closely related to CIN 3 cases with transforming HPV infection.

Conclusions

This study has shown that Raman spectroscopy can be successfully applied to the study of Thinprep cervical cytology samples from a cervical screening programme. Samples were prepared according to standard protocols and good quality Raman spectra were recorded from unstained single cervical cells on glass slides. Excellent sensitivity and specificity values were obtained particularly when CIN rather than SIL terminology was used to classify the samples. This suggests that the HSIL category is quite heterogeneous with CIN2 cases being biochemically different to CIN3 cases.

Acknowledgments

Financial support from the Dublin Institute of Technology Fiosraigh Research Excellence Scheme is gratefully acknowledged.

References

1. L. A. Torre, F. Bray, R. L. Siegel, J. Ferlay, J. Lortet-Tieulent and A. Jemal, *CA Cancer J Clin*, 2015, **65**, 87-108.
2. J. M. Walboomers, M. V. Jacobs, M. M. Manos, F. X. Bosch, J. A. Kummer, K. V. Shah, P. J. Snijders, J. Peto, C. J. Meijer and N. Munoz, *J Pathol*, 1999, **189**, 12-19.
3. E. L. Franco, N. F. Schlecht and D. Saslow, *Cancer J*, 2003, **9**, 348-359.
4. H. M. Shingleton, R. M. Richart, J. Wiener and D. Spiro, *Cancer Res*, 1968, **28**, 695-706.
5. D. Solomon, D. Davey, R. Kurman, A. Moriarty, D. O'Connor, M. Prey, S. Raab, M. Sherman, D. Wilbur, T. Wright, Jr. and N. Young, *JAMA*, 2002, **287**, 2114-2119.
6. T. M. Darragh, T. J. Colgan, J. T. Cox, D. S. Heller, M. R. Henry, R. D. Luff, T. McCalmont, R. Nayar, J. M. Palefsky, M. H. Stoler, E. J. Wilkinson, R. J. Zaino and D. C. Wilbur, *J Low Genit Tract Dis*, 2012, **16**, 205-242.
7. N. C. S. Programmes, *Achievable standards, Benchmarks for reporting, and Criteria for evaluating cervical cytopathology.*, NHS CSP Publication No 1. , Sheffield, 3rd edn., 2013.
8. L. G. Koss and M. R. Melamed, *Koss' Diagnostic Cytology and Its Histopathologic Bases*, Lippincott Williams & Wilkins, Philadelphia., Fifth Edit. edn., 2006.
9. H. C. Kitchener, R. Blanks, H. Cubie, M. Desai, G. Dunn, R. Legood, A. Gray, Z. Sadique and S. Moss, *Health Technol Assess*, 2011, **15**, iii-iv, ix-xi, 1-170.
10. M. Diem, A. Mazur, K. Lenau, J. Schubert, B. Bird, M. Miljkovic, C. Krafft and J. Popp, *J Biophotonics*, 2013, **6**, 855-886.
11. K. Kong, C. Kendall, N. Stone and I. Notingher, *Adv Drug Deliv Rev*, 2015, **89**, 121-134.
12. F. M. Lyng, D. Traynor, I. R. Ramos, F. Bonnier and H. J. Byrne, *Anal Bioanal Chem*, 2015, **407**, 8279-8289.
13. M. Fung Kee Fung, M. Senterman, P. Eid, W. Faught, N. Z. Mikhael and P. T. Wong, *Gynecol Oncol*, 1997, **66**, 10-15.

14. S. Neviliappan, L. Fang Kan, T. Tiang Lee Walter, S. Arulkumaran and P. T. T. Wong, *Gynecol Oncol*, 2002, **85**, 170-174.

15. P. T. Wong, R. K. Wong, T. A. Caputo, T. A. Godwin and B. Rigas, *Proc Natl Acad Sci U S A*, 1991, **88**, 10988-10992.

16. H. M. Yazdi, M. A. Bertrand and P. T. Wong, *Acta Cytol*, 1996, **40**, 664-668.

17. P. T. T. Wong, M. K. Senterman, P. Jackli, R. K. Wong, S. Salib, C. E. Campbell, R. Feigel, W. Faught and M. Fung Kee Fung, *Biopolymers*, 2002, **67**, 376-386.

18. L. Chiriboga, P. Xie, V. Vigorita, D. Zarou, D. Zakim and M. Diem, *Biospectroscopy*, 1998, **4**, 55-59.

19. M. A. Cohenford, T. A. Godwin, F. Cahn, P. Bhandare, T. A. Caputo and B. Rigas, *Gynecol Oncol*, 1997, **66**, 59-65.

20. M. Diem, L. Chiriboga, P. Lasch and A. Pacifico, *Biopolymers*, 2002, **67**, 349-353.

21. M. J. Romeo, M. A. Quinn, F. R. Burden and D. McNaughton, *Biopolymers*, 2002, **67**, 362-366.

22. B. R. Wood, M. A. Quinn, B. Tait, M. Ashdown, T. Hislop, M. Romeo and D. McNaughton, *Biospectroscopy*, 1998, **4**, 75-91.

23. M. A. Cohenford and B. Rigas, *Proc Natl Acad Sci U S A*, 1998, **95**, 15327-15332.

24. J. M. Schubert, B. Bird, K. Papamarkakis, M. Miljkovic, K. Bedrossian, N. Laver and M. Diem, *Lab Invest*, 2010, **90**, 1068-1077.

25. N. C. Purandare, Patel, II, J. Trevisan, N. Bolger, R. Kelehan, G. von Bunau, P. L. Martin-Hirsch, W. J. Prendiville and F. L. Martin, *Analyst*, 2013, **138**, 3909-3916.

26. K. Gajjar, A. A. Ahmadzai, G. Valasoulis, J. Trevisan, C. Founta, M. Nasioutziki, A. Loufopoulos, M. Kyrgiou, S. M. Stasinou, P. Karakitsos, E. Paraskevaidis, B. Da Gama-Rose, P. L. Martin-Hirsch and F. L. Martin, *PLoS One*, 2014, **9**.

27. E. Vargis, Y.-W. Tang, D. Khabele and A. Mahadevan-Jansen, *Transl Oncol*, 2012, **5**, 172-179.

28. S. Rubina, Amita, M., Kedar, K.D., Bharat, R., Krishna, C.M. , *Vibrational Spectroscopy*, 2013, **68**, 115–121.

29. F. Bonnier, Traynor, D., Kearney, P., Clarke, C., Knief, P., Martin, C., O'Leary, J.J., Byrne, H.J. and Lyng, F., , *Anal. Methods*, 2014, **6**.

30. H. J. Byrne, M. Baranska, G. J. Puppels, N. Stone, B. Wood, K. M. Gough, P. Lasch, P. Heraud, J. Sulé-Suso and G. D. Sockalingum, *Analyst*, 2015, **140**, 2066 - 2073.

31. P. Knief, PhD, Dublin Institute of Technology, 2010.

32. O. Ibrahim, A. Maguire, A.D. Meade, S. Flint, H. J. Byrne and F. M. Lyng, *Analytical Methods*, 2015.

33. Z. Movasaghi, S. Rehman and I. U. Rehman, *Appl. Spectrosc. Rev.*, 2007, **42**, 493–541.

34. C. M. Krishna, G. D. Sockalingum, B. M. Vadhiraja, K. Maheedhar, A.C.K.Rao, L. Rao, L. Venteo, M. Plutot, D. J. Fernandes, M.S.Vidyasagar, B. V. B. Kartha and M. Manfait, *Biopolymers* 2006, **85**, 214–221.

35. F. M. Lyng, E. O. Faolain, J. Conroy, A. D. Meade, P. Knief, B. Duffy, M. B. Hunter, J. M. Byrne, P. Kelehan and H. J. Byrne, *Exp Mol Pathol*, 2007, **82**, 121-129.

36. N. Rashid, H. Nawaz, K. W. Poon, F. Bonnier, S. Bakhiet, C. Martin, J. J. O'Leary, H. J. Byrne and F. M. Lyng, *Exp Mol Pathol*, 2014, **97**, 554-564.

37. K. M. Tan, C. S. Herrington and C. T. Brown, *J Biophotonics*, 2011, **4**, 40-48.

38. H. Griffin, Y. Soneji, R. Van Baars, R. Arora, D. Jenkins, M. van de Sandt, Z. Wu, W. Quint, R. Jach, K. Okon, H. Huras, A. Singer and J. Doorbar, *Mod Pathol*, 2015, **28**, 977-993.

Figure Legends

Figure 1 a) Mean Raman spectra from negative, LSIL and HSIL cervical cytology samples. Shading denotes the standard deviation, b) 1318/1339 cm^{-1} peak ratios for negative, LSIL and HSIL cervical cytology samples.

Figure 2 a) PCA scatterplot, b) PC1 loading and c) PC2 loading of negative, LSIL and HSIL cervical cytology samples.

Figure 3 a) Mean Raman spectra from CIN 2 and CIN 3 cervical cytology samples. Shading denotes the standard deviation, b) PCA scatterplot for negative, CIN 1, CIN 2 and CIN 3 cervical cytology samples.

Figure 4 a) PCA scatterplot and b) PC1 loading for CIN 1 and CIN 2 cervical cytology samples, c) PCA scatterplot and d) PC1 loading for CIN 1 and CIN 3 cervical cytology samples, e) PCA scatterplot and f) PC3 loading for CIN 2 and CIN 3 cervical cytology samples.

Table 1 Summary of the different cervical cytology / histology reporting systems

Cervical cytology / histology reporting systems			
CIN[1]	**BSCC[2] (1996)**	**SIL[3] (Bethesda) / CAP[4] / ASCCP[5]**	**BSCC (2013)**
1	Mild dyskaryosis	LSIL[6]	Low grade dyskaryosis
2	Moderate dyskaryosis	HSIL[7]	High grade dyskaryosis (moderate)
3	Severe dyskaryosis		High grade dyskaryosis (severe)

[1] Cervical intraepithelial neoplasia; [2] British Society for Clinical Cytology; [3] Squamous intraepithelial lesion; [4] College of American Pathologists; [5] American Society for Colposcopy and Cervical Pathology; [6] Low grade squamous intraepithelial lesion; [7] High grade squamous intraepithelial lesion

Table 2 Tentative peak assignments[28] for Raman spectra shown in Figure 1.

Raman shift (cm^{-1})	Assignment
621	C-C twisting mode of phenylalanine (proteins)
645	C-C twisting mode of phenylalanine (proteins)
722	Adenine
786	DNA: O-P-O; Pyrimidine ring breathing mode
828	Phosphodiester; O-P-O stretching DNA/RNA
856	Amino acid side chain vibrations of proline & Hydroxyproline, as well as a (C-C) vibration of the collagen backbone
1032	CH_2CH_3 bending modes of collagen & phospholipids; Phenylalanine of collagen; Proline (collagen assignment)
1093	Symmetric PO_2^- stretching vibration of the DNA backbone–phosphate backbone vibration as a marker mode for the DNA concentration C-N of proteins
1127	v(C-N)
1175/76	Cytosine, guanine
1209	Tryptophan & phenylalanine
1240	Amide III; Differences in collagen content; Asymmetric phosphate stretching modes
1246	Amide III (of collagen)
1307	CH_3/CH_2 twisting, wagging &/or bending mode of collagens & lipids
1318	Guanine (ring breathing modes of the DNA/RNA bases)-C-H deformation (protein); Amide III (α-helix)

1339	CH_2/CH_3 wagging & twisting mode in collagen, nucleic acid & tryptophan
1451	CH_2CH_3 deformation
1580	C-C stretching
1607	C=C phenylalanine, tyrosine
1617	C=C phenylalanine, tyrosine
1670	Amide I; C=C stretching vibrations; Amide I (anti-parallel β-sheet); n(C=C) trans, lipids, fatty acids

Table 3 Sensitivity and Specificity from Principal Component Analysis – Linear Discriminant Analysis (PCA-LDA) Classification of negative, LSIL and HSIL cervical cytology samples

	SIL classification		
	Negative	**LSIL**	**HSIL**
Sensitivity	100.00%	94.29%	86.05%
Specificity	97.22%	95.42%	100.00%

Table 4 Sensitivity and Specificity from Principal Component Analysis – Linear Discriminant Analysis (PCA-LDA) Classification of negative, CIN1, CIN2 and CIN3 cervical cytology samples

	CIN classification			
	Negative	CIN 1	CIN 2	CIN 3
Sensitivity	100.00%	94.29%	100.00%	90.91%
Specificity	97.37%	98.47%	97.24%	100.00%

a

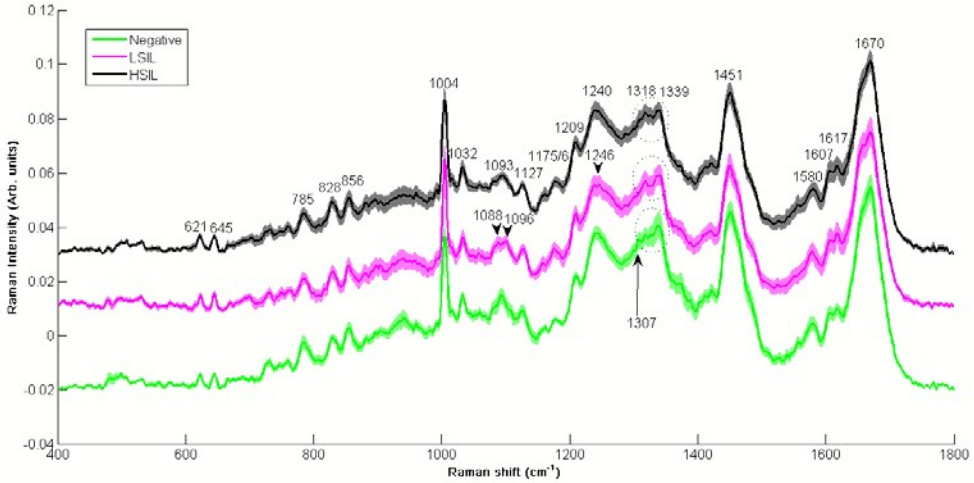

b

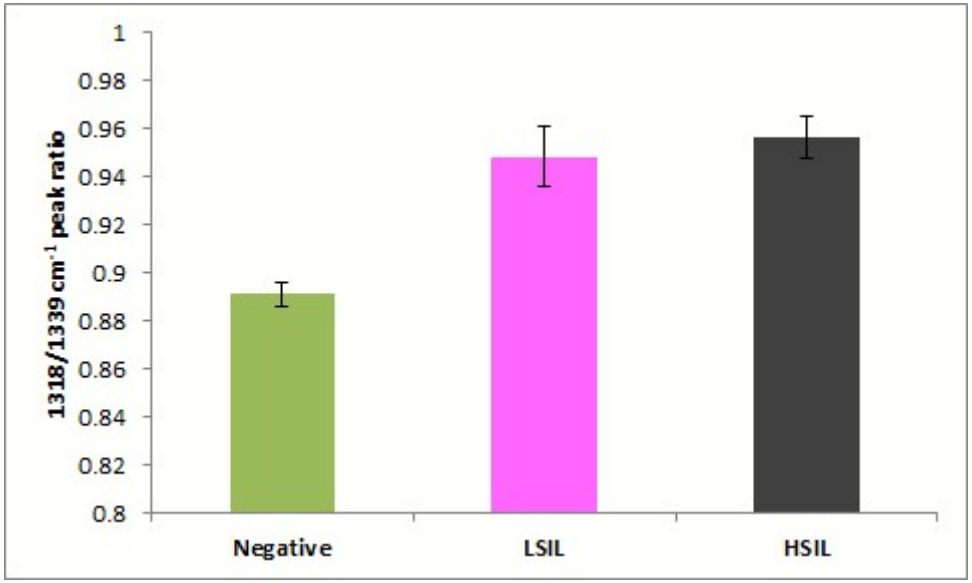

a

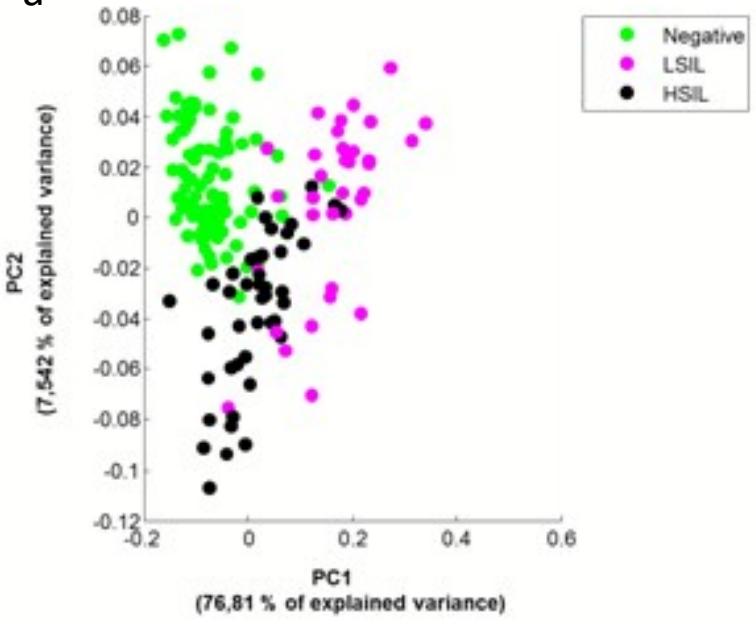

b

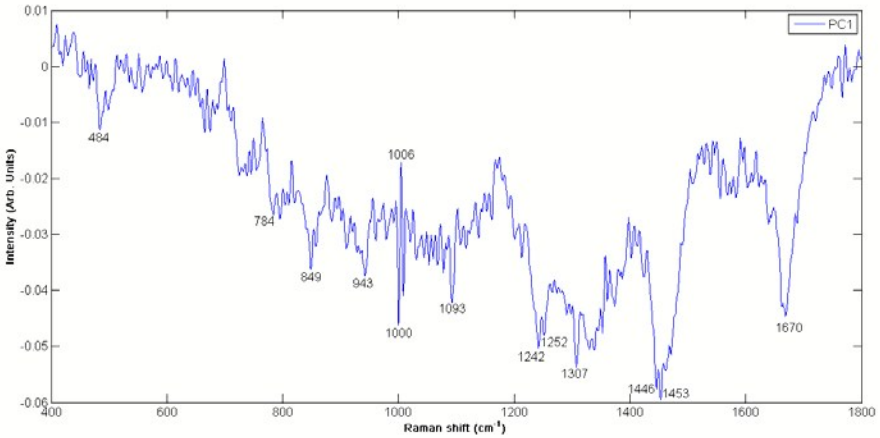

c

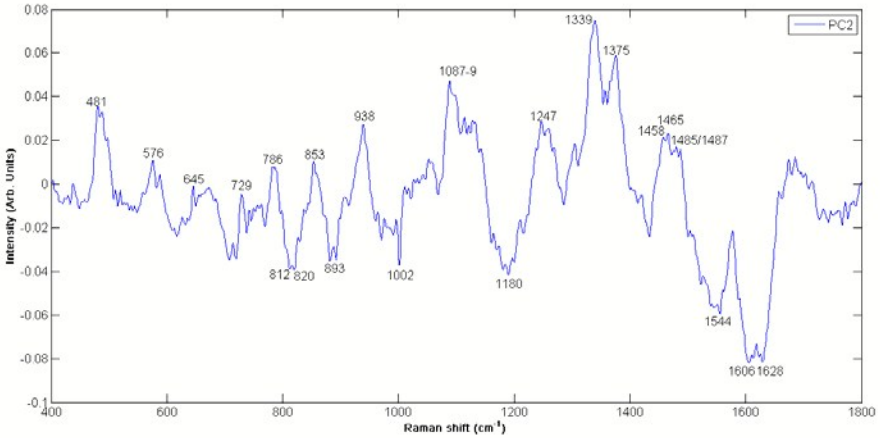

a

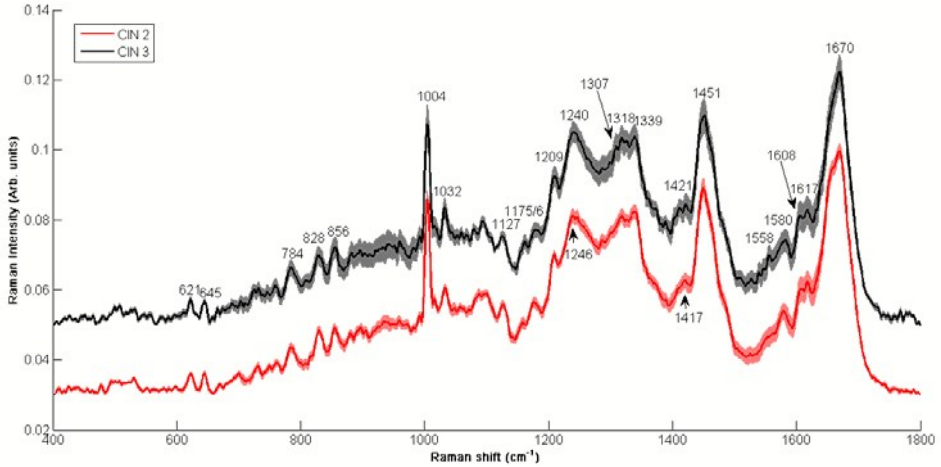

b